Liquid Crystals
Publication details, including instructions for authors and subscription information:
http://www.informaworld.com/smpp/title~content=t713926090

Atomic Force Microscopy of freely suspended liquid crystal films transferred to octadecyltriethoxysilane self-assembled monolayers

Baek-Woon Lee; Darren R. Link; Noel A. Clark

To cite this Article Lee, Baek-Woon , Link, Darren R. and Clark, Noel A.(2000) 'Atomic Force Microscopy of freely suspended liquid crystal films transferred to octadecyltriethoxysilane self-assembled monolayers', Liquid Crystals, 27: 4, 501 — 507

To link to this Article: DOI: 10.1080/026782900202697
URL: http://dx.doi.org/10.1080/026782900202697

LIQUID CRYSTALS, 2000, VOL. 27, NO. 4, 501–507

Atomic Force Microscopy of freely suspended liquid crystal films transferred to octadecyltriethoxysilane self-assembled monolayers

BAEK-WOON LEE, DARREN R. LINK and NOEL A. CLARK*

Ferroelectric Liquid Crystal Materials Research Center, Department of Physics,
University of Colorado, Boulder CO 80309, USA

(*Received 4 March 1999; in final form 14 October 1999; accepted 28 October 1999*)

Thin freely suspended films of 4-(2-methylbutyl)phenyl 4′-octylbiphenyl-4-carboxylate (8SI) in the smectic C phase were transferred to self-assembled monolayer coated glass and imaged by atomic force microscopy. Upon rapid cooling to room temperature, the smectic C quenches into a lamellar phase, exhibiting islands and single smectic layer steps. The surface of such films can be imaged with molecular resolution, revealing a partially disordered lattice of fixed molecular positions. Over a period of several days these films undergo a transition to a crystal phase having a different film morphology.

1. Introduction

Liquid crystals exhibit a variety of phases characterized by positional ordering intermediate between the free molecular translation in liquids and the molecular confinement in crystals. These include the smectics A and C, which are a lamellar stacking of two dimesional (2D) liquid layers, and the hexatic phases, which exhibit short range translational order combined with long range bond orientational order within the lamellar planes. Information about the positional ordering of molecules in such phases has come almost exclusively from X-ray scattering [1]. Here we show that the molecular organization in the planes of a lamellar liquid crystal phase can be effectively studied using scanning probe microscopy.

Scanning probe microscopy (SPM) offers an exciting new tool for the study of the structure of thermotropic LCs. However, in order to investigate the in-plane molecular organization, samples which are very thin and have the smectic layers parallel to the surface must be prepared, ideally on atomically smooth substrates. Graphite and mica have typically been employed for molecular resolution studies of LCs because of their atomically flat surfaces [2]. However, the strong interaction between these surfaces and thermotropic liquid crystal molecules controls the surface structure adopted, e.g. on graphite the LC forms 2D crystals which are commensurate with the surface honeycomb lattice [2, 3]. In this case collective properties intrinsic to the liquid crystal itself are not observed. Monolayers of lyotropic LC molecules have been deposited on mica using Langmuir–Blodgett (LB) techniques and imaged with molecular resolution [4].

Here we report molecular resolution atomic force microscopy (AFM) imaging of the in-plane molecular ordering in a thermotropic smectic liquid crystal phase. In these experiments, LC films of the liquid crystal 8SI a few layers thick were deposited on solid substrates using the transferred freely suspended film method [5, 6]. Smectic freely suspended films are quantized in thickness, consisting of integral numbers of smectic layers $N > 0$, and thus have well defined surfaces, a necessary condition for atomic or molecular resolution. Overney *et al.* [7] have demonstrated the utility of the transferred freely suspended film technique for AFM imaging, showing the basic features such as the layering and the molecular packing of crystalline methyl 4′-(*n*-heptyloxy)-biphenyl-4-carboxylate (I814) deposited onto hydrophobized quartz. Here we extend this technique to the study of partially ordered phases. The solid substrates for our experiments were float glass coated with octadecyltriethoxysilane self-assembled monolayers (SAMs), which provide an atomically smooth liquid-like structure of tightly packed hydrocarbon tails having low adhesive energy with the liquid crystal, desirable characteristics for AFM imaging of the LC in-plane structure. We expect the SAM surface to have the least possible influence on the liquid crystal structure among available substrates.

2. Experiments

In our experiments, transferred freely suspended films of 4-(2-methylbutyl)phenyl 4′-octylbiphenyl-4-carboxylate (8SI) on octadecyltriethoxysilane (OTE) SAMs were

---

*Author for correspondence;
e-mail: Noel.clark@colorado.edu

Liquid Crystals ISSN 0267-8292 print/ISSN 1366-5855 online © 2000 Taylor & Francis Ltd
http://www.tandf.co.uk/journals/tf/02678292.html

studied by AFM. Freely suspended films of 8SI at $T = 80°C$ in the smectic C phase were transferred to room temperature SAM-coated glasses, quenching into a lamellar smectic phase at room temperature. AFM images were obtained over a range of length scales and resolutions. The surface of the transferred films exhibited molecularly smooth surfaces which could be imaged with molecular resolution. The molecular resolution images show an in-plane lattice which is anisotropic, generally having one distinct direction having the best-defined periodicity. The other directions exhibit less order, a feature suggestive of an anisotropic lattice in which molecules are tilted with respect to the layer plane. Also observed is a periodic undulation of the smectic layers, having a wavelength $\lambda \sim 2000$ Å, possibly a result of in-plane compressive layer stress during the cooling process. These features of the lamellar smectic phase disappear over a 2–3 day period, with the deposited films passing through a phase transition to the bulk crystalline phase.

The chemical structure of 8SI is shown below.

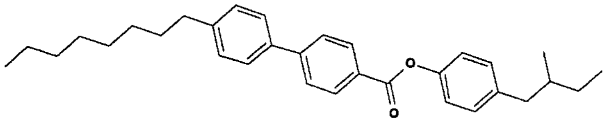

Bulk 8SI has the following phase sequence [8]:

I 140°C N 134°C SmA 82.5°C SmC 67.9°C SmI 62.0°C J 56.6°C G 50.5°C Cr.

For thin films, however, the phase sequence is quite different [9], e.g. for a 2-layer thick film [10]:

SmA 115°C SmC 77.5°C SmI 77.4°C SmF 63.5°C J.

The SmA–SmC transition occurs at a higher temperature in the thin film, as is often observed [11], a result of the tendency for the molecules in the surface layers to be tilted. At lower temperatures, however, the molecular positions in the films become more disordered than those in the bulk, an effect coming from enhanced fluctuations associated with the reduced dimensionality, as also found in other materials [10]. The films studied here, 5–10 layers thick, appear to have, like the bulk, a SmC–SmI–J phase sequence, i.e. the SmF phase is not seen.

8SI in the SmC phase was drawn across a $3 \times 7\,\mathrm{mm}^2$ rectangular hole in a cover glass housed in a temperature controlled oven (± 0.01°C), as shown in figure 1. Initially the film was usually several microns thick and had numerous circular island layers floating on it. To make it uniform and thinner, the film was heated near to the SmA–N transition and thinned [12] to 5–10 layers before transfer. The number of layers was determined by the measurement of the reflectivity of the film for incident He-Ne laser light. Since the reflectivity increases quadratically with the thickness, the number of the layers for thin films can be easily determined.

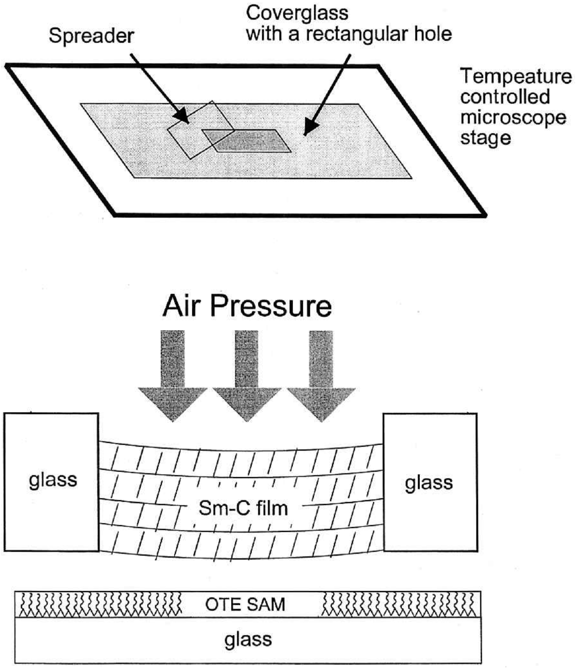

Figure 1. Schematic of the cell and transfer process for deposition of a freely suspended film onto a SAM-coated glass slide.

The SAMs were prepared with a 2 wt % solution of OTE in toluene with 0.5% butylamine as a catalyst [13]. Water wets the SAM coated glasses with a contact angle of about 110°, which is almost the same as that of octadecane. Thus the surface energy of the SAM coated glass is estimated to be $28\,\mathrm{mJ\,m^{-2}}$ and the interfacial energy with water is $52\,\mathrm{mJ\,m^{-2}}$ [14]. AFM of the SAM surface showed it to be molecularly smooth and rigid, but with no discernable molecular structure. In order to transfer an LC film to the SAM, the SAM was carefully placed within 200 µm of the film and a positive pressure differential was then applied to the side opposite from the film. The film bulged towards the SAM and transferred to it. While the transfer occurred at 80°C, the SAM substrate was kept at room temperature until the last moment to quench the film from the SmC phase. Then the sample was imaged at room temperature with a Nanoscope III AFM from Digital Instruments in contact mode. The K scanner (180 µm) was used for micron-sized images and the A scanner (800 nm) was used for molecular resolution images, both with silicon nitride (Si_3N_4) tips from Park Scientific Instruments, having a spring constant of $0.06\,\mathrm{N\,m^{-1}}$. The constant height mode turned out to yield better resolution and to inflict less damage to the films and was used for scans of scan size $< 200 \times 200\,\mathrm{nm}^2$. For other scans, the constant force mode was used.

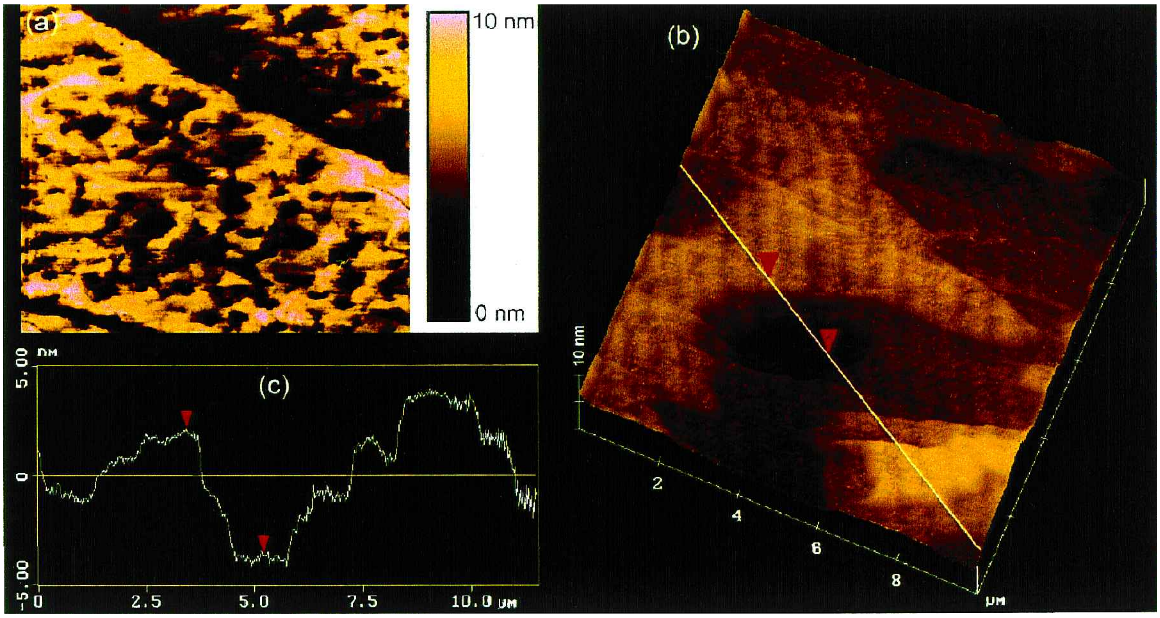

Figure 2. Large length scale AFM images of a transferred freely suspended film of 8SI, taken at room temperature shortly after rapid cooling from the SmC phase. The film quenches into a highly ordered lamellar smectic phase and the surface is covered with irregular shaped islands a few smectic layers in height. The profile shows the layer thickness to be ≅ 2.8 nm. (*a*) 50 × 100 µm^2 image; (*b*) 10 × 10 µm^2 image clearly showing the layer steps; (*c*) plot showing the cross section along the white line. Also evident is a periodic surface undulation.

Obtaining molecular resolution is most readily achieved when the surfaces being imaged are hard, flat, and well ordered. The major hurdle in the experiment was to prepare sufficiently hard films to withstand the loading force of AFM. Because of the finite smectic layer compressibility, films become effectively softer as their thickness increases, making imaging more difficult. Thick films of 8SI with $N > \cong 10$ did not yield molecular resolution even in the crystalline phase. With thin films, we were able to image the local in-plane order in the quenched films.

Images

Figures 2 and 3 show large length scale images of a transferred, freely suspended film of 8SI, obtained within the first few hours of transfer. The left image in figure 2 (*a*) is 50 × 100 µm^2. Although the film was uniformly a few layers thick before transfer, it now consists mostly of layered islands, typically 10 µm^2 in size. Cracks in otherwise flat layers also develop during the quench (figure 3). Figure 2 (*b*) clearly shows the film surface to be the surface of the smectic layers, the height difference between the two red arrows being 5.68 nm, which corresponds to 2.8 nm per step, comparable to the bulk layer spacing of 8SI [15]. The edges of the islands are not round as found in the SmC films, but they are not as sharp as the ones in a crystalline phase [7]. In addition to the

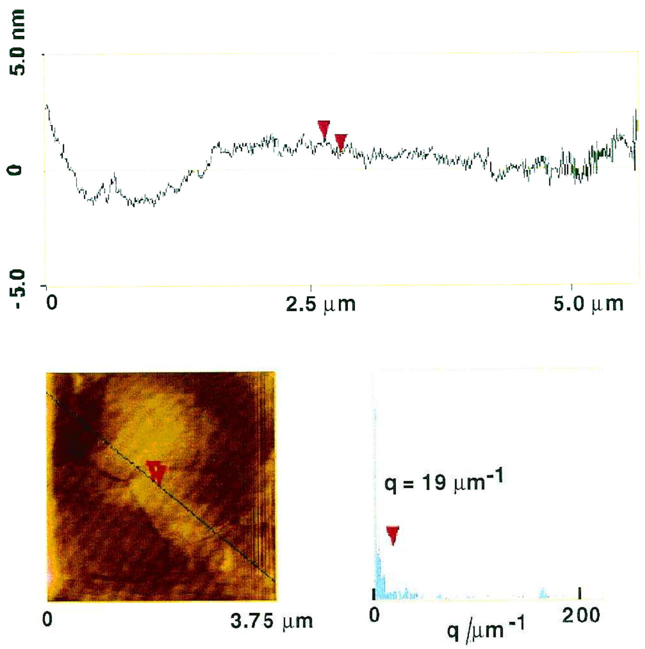

Figure 3. 4 × 4 µm^2 AFM image, showing $\delta h(s)$, a sectional surface height profile along the indicated line, and $\delta h(\mathbf{q})$, its one dimensional Fourier transform. The image, profile, and Fourier transform all yield evidence for a smooth surface undulation having an amplitude $\delta h \cong 0.6$ nm and a wavelength $\lambda \cong 0.33$ µm.

layering, these images show a smooth quasi-periodic height undulation having a wavelength $\lambda \cong 0.3\,\mu\text{m}$ and a peak-to-valley height of $\delta h \cong 1$ nm. This undulation is a ubiquitous feature of the large scale images in the films as quenched, with λ and δh both increasing as the film thickness increases. Figure 3 shows a profile $\delta h(\text{s})$ along the indicated line and its one dimensional Fourier transform $\delta h(\mathbf{q})$, indicating a period of undulation of $p = 2\pi/(19\,\mu\text{m}^{-1}) = 330$ nm.

Figure 4 presents in the leftmost column a series of molecular resolution images, $\delta h(x, y)$, of the two dimensional height variation of a transferred freely suspended film of 8SI, obtained by imaging layer surfaces such as those in figures 2 and 3 with the high-resolution scanner. The images of figure 4 show a region of a continuous lamellar layer surface at three resolutions, ranging from $10 \times 10\,\text{nm}^2$ to $30 \times 30\,\text{nm}^2$. In order to enhance the viewability of the molecular ordering, these images were

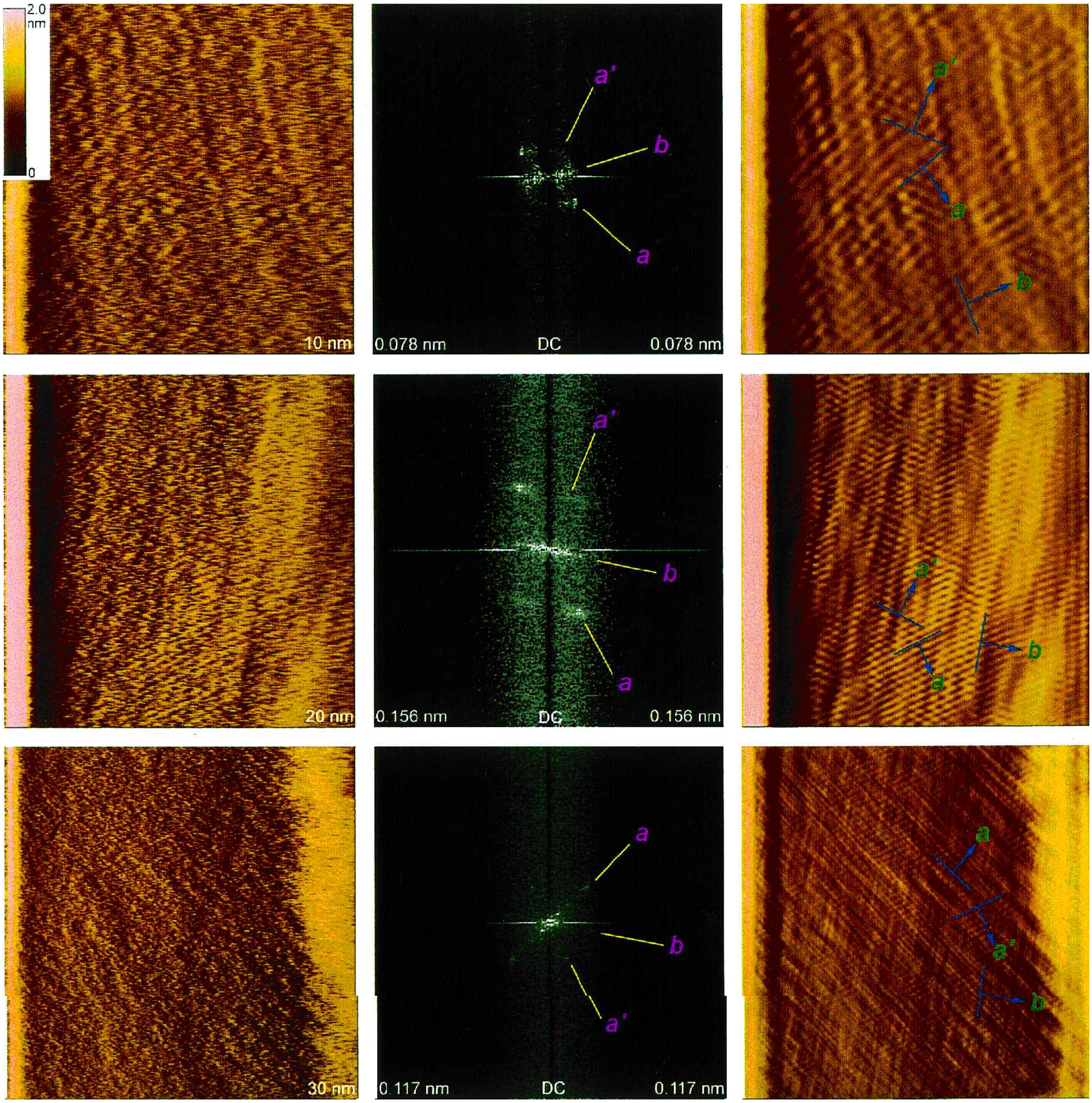

Figure 4. High resolution images of a layer surface of a preparation as in figures 2 and 3, shown at $10 \times 10\,\text{nm}^2$, $20 \times 20\,\text{nm}^2$, and $30 \times 30\text{nm}^2$ scale. The left column is the height image $\delta h(x, y)$, the centre column its two dimensional Fourier transform, $\delta h(\mathbf{q})$, and the right hand column $\delta h_{\text{f}}(x, y)$, the spatially filtered $\delta h(x, y)$. Two distinct sets of molecular rows, normal to **a** and **a**′, are evident in each of the images, one of which is better ordered (**a**, more visible with fewer dislocations). There is also a wrinkling of the surface with undulations on a molecular row scale, normal to the direction **b**. The wrinkling direction approximately bisects the angle between **a** and **a**′. The wrinkles appear to mediate the disorder of the **a**′ rows.

spatially filtered with the filtered result, $\delta h_f(x, y)$, shown in the right hand column. The filtering was carried out by calculating $\delta h(\mathbf{q})$, the two dimensional Fourier transform $\delta h(x, y)$ shown in the centre column, retaining only its distinct features (e.g. peaks and streaks), and then retransforming to obtain filtered images.

The images of the different areas and their Fourier transforms are qualitatively similar, exhibiting the following typical features:

(1) A lattice formed by two intersecting sets of rows (normal to the directions **a** and **a′** (orientations θ_a and $\theta_{a'}$), having row spacings d in the range $0.39 < d < 0.51$ nm, and an angle ψ between the rows in the range $45° < \psi < 67°$. These appear to be rows of molecules, having a lattice spacing in the range for in-plane packing of LC molecules. One or both of these sets of rows will generate a distinct peak in $\delta h(\mathbf{q})$.

(2) A series of peaks along a linear streak in $\delta h(\mathbf{q})$ [taken to be the direction **b** (orientation θ_b)], arising from a wave-like quasi-periodic buckling or disordering of the surface (wrinkle pattern) with the waves oriented normal to **b**. The length characteristic of the buckling is comparable to a few molecular row spacings, so that this buckling is distinct from the periodic macroscopic undulations in figures 2 and 3. The **b** direction approximately bisects ψ.

Generally one of the sets of rows is continuous with relatively few dislocations in a $20 \times 20\,\mathrm{nm}^2$ area, whereas the other set is quite strongly defected. The continuous rows are typically the best defined in the image and produce the most distinct Bragg peaks in $\delta h(\mathbf{q})$. This defecting is correlated with the quasi-periodic distortion of the surface generating feature (2).

Attempts to observe the layer steps in figures 2 and 3 with molecular resolution were not successful. The layers are sufficiently plastic that the presence of the tip displaces the position of the layer step in the top layers. This ‘sweeping’ of the layer edge by the tip was observed in scans of several hundred nanometers.

As we will discuss next, the AFM images of figure 4 are indicative of a J phase molecular arangement. However, the appearance, under AFM imaging, of the surface of transferred freely suspended 8SI films changes dramatically as time passes after transfer. This change is a result of crystallization, the J to Cr phase transition, leading to a surface covered by crescent-shaped bent crystallites, shown in figure 5, which are much thicker than the layered islands, indicating that they must form at the expense of thinning of the rest of the film area. The time required for this transformation increases with decreasing film thickness, becoming as long as 2–3 days for the thinnest films. Thicker films have a higher crystallite density. The surfaces of these crystallites were not flat and could not be imaged with molecular resolution.

4. Discussion

The AFM images show that upon rapid cooling from the SmC phase, the deposited freely suspended films are quenched into a lamellar phase, characterized by 2.8 nm thick layers, and, at molecular resolution, observable in-plane ordering. Since the molecules are tilted relative to the layer normal in all of the smectic phases below the SmC deposition temperature, we expect that the molecules will be tilted in the room temperature quenched lamellar structure, i.e. that it be either a tilted hexatic phase (smectic F or I), or a phase with crystalline in-plane order (G or J), shown schematically in figure 6. The appearance of a dominant set of molecular rows in the high-resolution images and their Fourier transforms is strongly suggestive of the smectic I phase or the J phase, in which the molecules are tilted in the direction of nearest neighbours, producing a unique set of lowest order rows, as opposed to the situation in smectic F, where there are two equivalent sets. In the dominant (**a**) row direction viewing the images edge on and sighting down the rows shows them to be defect free over areas as large as 5 nm × 5 nm square. The secondary (**a′**) rows, by contrast are much more defected, exhibiting a high density of edge dislocations and definitely short ranged order. The defects in the **a′** row patterns are clearly correlated with the (**b**) wrinkle pattern, the rows shifting as bands in the wrinkle pattern are crossed. There is no sign of the third set of rows that would be expected in a triangular lattice of untilted molecules. The wrinkle pattern orientation is clearly correlated in orientation relative to the **a** and **a′** directions, with the direction of **b**, the normal to the wrinkles, bisecting that of **a** and **a′**. The angular separations between these three directions vary from place to place on the film, presumably a result of distortion of the tip during scanning. The observation of inequivalence among the three sets of lowest order rows that should exist for a low symmetry 2D crystal indicates that the local order is anisotropic, which is consistent with molecules being tilted in the quenched structure. Having a single set of well defined rows is suggestive of the smectic I phase or the J phase, where the molecules are tilted towards their nearest neighbours, i.e. in the direction of a lowest order row which would enhance the apparent continuity of that set of rows. These observations indicate that such molecular resolution images may be useful in the identification of the more ordered LC phases.

The long wavelength layer undulation is probably generated at the time of transfer, either by the temperature quench or reduction in fluctuations accompanying

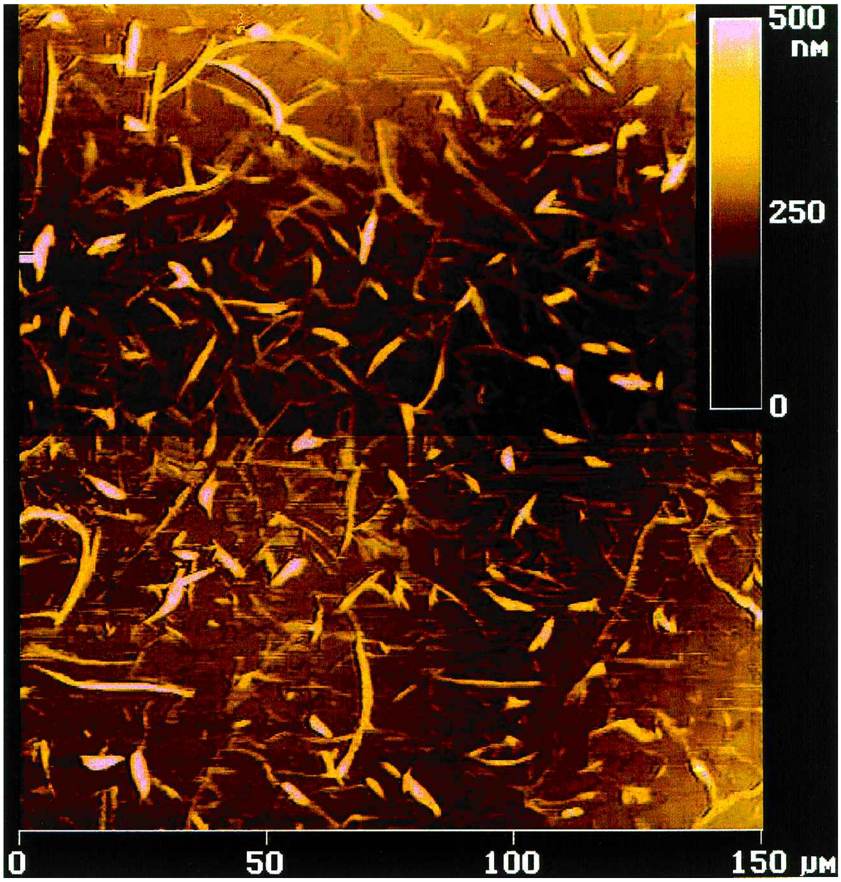

Figure 5. An AFM image of a transferred freely suspended film of 8SI, 3 days after transfer. The film has crystallized, forming curved crystallites on the film surface. The crystallites are much thicker than the islands of figure 2, indicating that they must form at the expense of thinning of the rest of the film area.

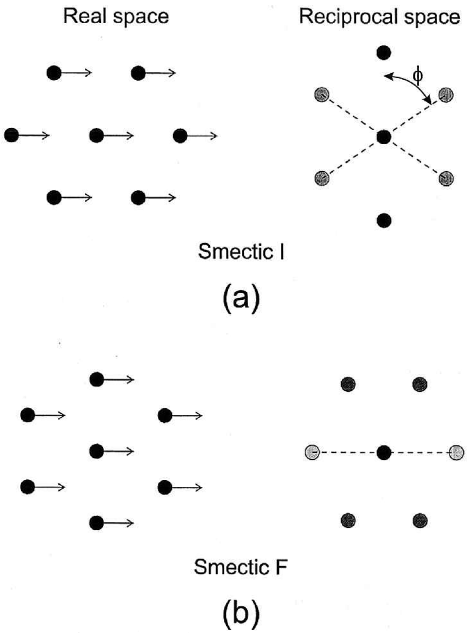

Figure 6. Schematic of the structures of the tilted smectic phases having at least local in-plane order. The appearance of a single well developed set of rows in the images suggests that the in-plane structure is that of the smectic I phase or the J phase.

adhesion to the smooth solid substrate causing the layers to increase in area. The AFM images in figures 2 and 3 show the undulation, having a period of ~300 nm and an amplitude of ~0.5 nm. The buckling suggests an in-plane compressive layer stress which is relieved partially by the undulation.

This work was supported by NSF MRSEC Grant DMR 98-09555, NSF Grant DMR 96-14061, and NASA Grant NAG3-1846.

References

[1] Pershan, P. S., 1988, *Structure of Liquid Crystal Phases* (Singapore: World, Scientific).
[2] Smith, D. P. E., Horber, H., Gerber, Ch., and Binnig, G., 1989, *Science*, **245,** 43.
[3] Parks, D. C., Clark, N. A., Walba D. M., and Beale, P. D., 1993, *Phys. Rev. Lett.*, **70,** 607.
[4] Zasadzinski, J. A., Viswanathan, R., Madsen, L., Garnaes, J., and Schwartz, D. K., 1994, *Science*, **263,** 1726.
[5] Maclennan, J. E., Decher, G., and Sohling, U., 1991, *Appl. Phys. Lett.*, **59,** 917.
[6] Decher, G., Maclennan, J. E., Reibel, J., and Sohling, U., 1991, *Adv. Mat.*, **3,** 617.
[7] Overney, R. M., Meyer, E., Frommer, J., Guntherodt, H.-J., Decher, G., Reibel, J., and Sohling, U., 1993, *Langmuir*, **9,** 341.

[8] Shao, R., Zhuang Z., and Clark, N. A., 1991, *Ferroelectrics*, **122,** 213.

[9] Sirota, E. B., Pershan, P. S., Sorensen, L. B., and Collett, J., 1985, *Phys. Rev. Lett.*, **55,** 2039.

[10] Van Winkle, D. H., Dierker, S. B., and Clark, N. A., 1989, *J. chem. Phys.*, **91,** 5212.

[11] Heinekamp, S., Pelcovits, R. A., Fontes, E., Chen, E. Yi., Pindak, R., and Meyer, R. B., 1984, *Phys. Rev. Lett.*, **52,** 1017.

[12] Stoebe, T., Mach, P., and Huang, C. C., 1994, *Phys. Rev. Lett.*, **73,** 1384.

[13] Mooney, J. F., Hunt, A. J., McIntosh, J. R., Liberko, C. A., Walba, D. M., and Rogers, C. T., 1996, *Proc. natl. Acad. Sci. USA*, **93,** 12 287.

[14] Israelachvili, J. N., 1991, in *Intermolecular & Surface Forces* (San Diego: Academic Press), p. 315.

[15] Pzedmojski, J., Gerlotka, S., Wisniewski, R., Pura, B., and Zajak, W., 1989, *Ferroelectrics*, **92,** 345.